

Novel PdAu@Au/C Core–Shell Catalyst: Superior Activity and Selectivity in Formic Acid Decomposition for Hydrogen Generation

Yunjie Huang,^{†,‡} Xiaochun Zhou,^{†,‡} Min Yin,^{†,‡} Changpeng Liu,[†] and Wei Xing*[†]

[†]State Key Laboratory of Electroanalytical Chemistry, Changchun Institute of Applied Chemistry, Chinese Academy of Sciences, 5625 Renmin Street, Changchun 130022, P. R. China, and [‡]Graduate University of Chinese Academy of Sciences, Beijing 10039, P. R. China.

Received February 1, 2010. Revised Manuscript Received July 21, 2010

A novel PdAu bimetallic catalyst with a PdAu@Au core–shell nanostructure supported on carbon was facilely synthesized by a simultaneous reduction method without using any stabilizer. The structure was characterized by cyclic voltammetry, X-ray diffraction, transmission electron microscopy (TEM), and high-angle annular dark-field scanning TEM combining with X-ray energy-dispersive spectroscopy. The obtained catalyst was applied in hydrogen generation from formic acid decomposition. Results show that the structured bimetallic catalyst possesses superior activity, high selectivity, and stability at low temperature. The reforming gas from formic acid decomposition contains only 30 ppm of CO and can be used directly in fuel cell.

Introduction

Hydrogen is one of the most important clean energy carriers for sustainable development of the future world. In particular, when clean energy conversion devices such as fuel cells are feasible, the hydrogen economy will become a reality. With respect to this, hydrogen generation from renewable sources will be of high significance. Recently, the decomposition of formic acid has been intensely investigated for hydrogen generation, particularly in the area of reforming catalyst development.^{1–5} For example, Ru-based homogeneous catalysts have been reported to have high performance for the formic acid decomposition at near-ambient temperatures.^{1,2} On the other hand, some heterogeneous noble metal catalysts such as Pd have also been explored.^{6–8} Unfortunately, those heterogeneous catalysts are easily deactivated because of the poisoning intermediates. Generally, the heterogeneous catalyst is easy to use widely because it is facile to be controlled, retrieved, and recycled. Therefore, there is a strong desire to develop heterogeneous catalysts with high activity and selectivity for the formic acid decomposition under mild conditions.

Bimetallic materials have attracted considerable attention because of their different catalytic, electronic, and

optical properties compared to those of monometallic components.^{9–12} Among the various bimetallic materials, PdAu has been intensively investigated and employed as catalyst for many important applications such as CO oxidation,¹³ aldehyde preparation from alcohol oxidation,¹⁴ hydrodesulfurization of thiophene,¹⁵ and hydrogen peroxide synthesis.¹⁶ It has been recognized that controlling the bimetallic structures plays a critical role in achieving their favorite properties.^{17–24} For example, bimetallic core–shell structure that contains an inner core of one metal element and an external shell of the other metal element has shown some unique physical and

*Corresponding author. E-mail: xingwei@ciac.jl.cn.

- (1) Beller, M.; Loges, B.; Boddien, A.; Junge, H.; Beller, M. *Angew. Chem., Int. Ed.* **2008**, *47*, 3962.
- (2) Laurenczy, G.; Fellay, C.; Dyson, P. J.; Laurenczy, G. *Angew. Chem., Int. Ed.* **2008**, *47*, 3966.
- (3) Zhou, X. C.; Huang, Y. J.; Xing, W.; Liu, C. P.; Liao, J. H.; Lu, T. H. *Chem. Commun.* **2008**, 3540.
- (4) Ojeda, M.; Iglesia, E. *Angew. Chem., Int. Ed.* **2009**, *48*, 4800.
- (5) Ting, S. W.; Cheng, S. A.; Tsang, K. Y.; van der Laak, N.; Chan, K. Y. *Chem. Commun.* **2009**, 7333.
- (6) Ruthven, D. M.; Upadhye, R. S. *J. Catal.* **1971**, *21*, 39.
- (7) Hill, S. P.; Winterbottom, J. M. *J. Chem. Technol. Biotechnol.* **1988**, *41*, 121.
- (8) Akiya, N.; Savage, P. E. *AIChE J.* **1998**, *44*, 405.

- (9) Toshima, N.; Yonezawa, T. *New J. Chem.* **1998**, *22*, 1179.
- (10) Ferrando, R.; Jellinek, J.; Johnston, R. L. *Chem. Rev.* **2008**, *108*, 845.
- (11) Adams, B. D.; Wu, G. S.; Nigrio, S.; Chen, A. C. *J. Am. Chem. Soc.* **2009**, *131*, 6930.
- (12) Knecht, M. R.; Weir, M. G.; Frenkel, A. I.; Crooks, R. M. *Chem. Mater.* **2008**, *20*, 1019–1028.
- (13) Gao, F.; Wang, Y. L.; Goodman, D. W. *J. Am. Chem. Soc.* **2009**, *131*, 5734.
- (14) Enache, D. I.; Edwards, J. K.; Landon, P.; Solsona-Espriu, B.; Carley, A. F.; Herzing, A. A.; Watanabe, M.; Kiely, C. J.; Knight, D. W.; Hutchings, G. J. *Science* **2006**, *311*, 362.
- (15) Venezia, A. M.; La Parola, V.; Nicoli, V.; Deganello, G. *J. Catal.* **2002**, *212*, 56.
- (16) Edwards, J. K.; Solsona, B. E.; Landon, P.; Carley, A. F.; Herzing, A.; Kiely, C. J.; Hutchings, G. J. *J. Catal.* **2005**, *236*, 69.
- (17) Zhou, S. H.; Jackson, G. S.; Eichhorn, B. *Adv. Funct. Mater.* **2007**, *17*, 3099.
- (18) Alayoglu, S.; Eichhorn, B. *J. Am. Chem. Soc.* **2008**, *130*, 17479.
- (19) Sanchez, S. I.; Small, M. W.; Zuo, J. M.; Nuzzo, R. G. *J. Am. Chem. Soc.* **2009**, *131*, 8683.
- (20) Sun, Y. G.; Tao, Z. L.; Chen, J.; Herricks, T.; Xia, Y. N. *J. Am. Chem. Soc.* **2004**, *126*, 5940.
- (21) Luo, J.; Wang, L.; Mott, D.; Njoki, P. N.; Lin, Y.; He, T.; Xu, Z.; Wanjana, B. N.; Lim, I. I. S.; Zhong, C. J. *Adv. Mater.* **2008**, *20*, 4342.
- (22) Tao, F.; Grass, M. E.; Zhang, Y. W.; Butcher, D. R.; Renzas, J. R.; Liu, Z.; Chung, J. Y.; Mun, B. S.; Salmeron, M.; Somorjai, G. A. *Science* **2008**, *322*, 932.
- (23) Lei, Y.; Chim, W. K. *J. Am. Chem. Soc.* **2005**, *127*, 1487.
- (24) Kobayashi, H.; Yamauchi, M.; Kitagawa, H.; Kubota, Y.; Kato, K.; Takata, M. *J. Am. Chem. Soc.* **2008**, *130*, 1818.

chemical properties.^{21–24} To explore high catalytic properties, the studies on the PdAu catalyst have been directed toward the preparation method for designing special structures. Using poly(*N*-vinyl-2-pyrrolidone) as a stabilizing agent, Toshima et al.^{25–27} prepared almost all the possible structures of PdAu such as core–shell, clusters to clusters, random alloy, and mixture. These structures could be controlled only by changing the reduction method and molar ratio of Pd/Au. It was found that the dendrimer could be also used as a stabilizer for designing the microstructure of the PdAu bimetallic system.^{28–30} Teng et al.³¹ observed that the structure of PdAu nanoparticles could be controlled by the galvanic replacement reaction between Pd ultrathin nanowires and AuCl₃. The Pd nanowires were first changed to the PdAu alloy with a structure of Pd-rich shell/Au-rich core, then to the random PdAu alloy and finally to the complete Au nanoparticles. The heat treatment of the as-prepared PdAu bimetallic catalyst was also demonstrated to be an effective method for tuning the microstructure of PdAu.^{32,33} During the calcinations of PdAu particles in the atmosphere, the Pd had a tendency to be exposed on the particle surface, which resulted in a structure of Au-rich core/Pd-rich shell. However, the subsequent reduction of a previously calcined catalyst brought out many particles with Pd-rich core/Au-rich shell morphology.³² Recently, a three-layer structure was obtained in a core–shell system by a successive reduction of monometallic element. This core–shell nanoparticle was characterized as a PdAu alloy inner core, an Au-rich intermediate layer and a Pd-rich outer shell.³⁴

In this paper, a novel core–shell nanostructure of PdAu was prepared by a facile simultaneous reduction method without adding any stabilizing agent. It contains a core of PdAu alloy and an Au shell. More important, the PdAu bimetal system is supported on carbon and can be used directly as a heterogeneous catalyst without further treatment. The most remarkable finding is that the structured PdAu bimetallic catalyst shows superior activity, high selectivity, and stability in formic acid decomposition for hydrogen generation at low temperature.

Experimental Section

Catalyst Preparation. The carbon-supported PdAu bimetallic catalyst was synthesized as follows. For the first step, 108 mg of Vulcan XC-72 carbon powder was ultrasonically dispersed in 200 mL of water and subsequently mixed with 12 mM H₂AuCl₄ and 36 mM H₂PdCl₄ solution. The Au loading in the catalyst was expected to be 56 wt % and 5.6 times higher than that of Pd. The freshly prepared 150 mL of 70 mM NaBH₄ solution was dropped into the above suspension. The mixture was stirred for another 8 h at room temperature in order to deposit the bimetal onto the support absolutely. Finally, the desired catalyst from the suspension was filtered and washed with the hot triply distilled water and then dried in vacuum at 80 °C overnight. For comparison, the monometallic catalysts of Pd/C and Au/C with a corresponding metal loading of 10 and 56 wt % were also prepared separately using the same method.

Physical Characterizations for the Catalysts. Transmission electron microscopy (TEM) was performed using a Philips TECNAI G2 microscope with an acceleration voltage of 200 kV. Structural analysis of the selected particles was performed in scanning TEM (STEM) mode in combination with X-ray energy-dispersive spectroscopy (EDS) in the same microscope. STEM image was recorded with a high-angle annular dark-field (HAADF) detector. EDS profile scan data were collected using a collection time of 100 ms. Integrated intensities obtained from the C–K, Pd–L and Au–L were used for quantification of carbon and the two metals, respectively. The sample for the microscopic characterizations was prepared by spreading a drop of colloidal solution onto a carbon film supported by a Cu grid and subsequent drying in vacuum. X-ray diffraction (XRD, Bruker D8 Advance, Germany) measurements were carried out with a scanning speed of 2 degree min⁻¹. The inductively coupled plasma optical emission spectrometry (ICP-OES, Thermo (Icap6300, USA)) was employed for elemental analysis of the PdAu/C catalyst before and after use. Fourier-transform infrared spectroscopy (FT-IR, Bruker IFS 66 V/S, Germany) was used for CO determination. In the characterization, a cylindrical vessel with a volume of about 30 mL was used. First, the vessel was vacuumized by a pump. Then, the gas for detection was injected into the vessel by an injector until the vessel was full of the gas at an atmospheric pressure. Finally, the FT-IR spectra of the gas were recorded with a scan resolution of 2 cm⁻¹. Thirty-two cycles were made before the results come out. For the blank situation, N₂ was used before the measurement.

Electrochemical Characterizations for the Catalysts. For working electrode preparation, a glassy carbon disk electrode with a geometric area of 0.1256 cm² was used as the substrate on which a catalyst layer containing the synthesized catalyst and Nafion ionomer was coated. For the electrode coating process, 5 mg of the catalyst was dispersed ultrasonically in ethanol (1 mL) with Nafion solution (5%, 50 μL) to form the catalyst ink. Then, 10 μL of this ink was pipetted on the polished glassy carbon electrode surface uniformly. Thus, after the solvent was volatilized in air, a catalyst-coated working electrode was produced and ready for the measurements. For electrochemical measurements, a three-electrode cell was used, which consisted of a catalyst-coated working electrode, a Pt coil counter electrode, and an Ag/AgCl reference electrode. All the electrochemical characterizations were recorded using a Princeton Applied Research model 273 Potentiostat/Galvanostat at room temperature. Cyclic voltammetry was carried out in an aqueous solution of 0.5 M H₂SO₄. The solution was bubbled with a pure

- (25) Toshima, N.; Harada, M.; Yamazaki, Y.; Asakura, K. *J. Phys. Chem.* **1992**, *96*, 9927.
- (26) Harada, M.; Asakura, K.; Toshima, N. *J. Phys. Chem.* **1993**, *97*, 5103.
- (27) Shiraishi, Y.; Ikenaga, D.; Toshima, N. *Aust. J. Chem.* **2003**, *56*, 1025.
- (28) Scott, R. W. J.; Wilson, O. M.; Oh, S. K.; Kenik, E. A.; Crooks, R. M. *J. Am. Chem. Soc.* **2004**, *126*, 15583.
- (29) Scott, R. W. J.; Sivadinarayana, C.; Wilson, O. M.; Yan, Z.; Goodman, D. W.; Crooks, R. M. *J. Am. Chem. Soc.* **2005**, *127*, 1380–1381.
- (30) Weir, M. G.; Knecht, M. R.; Frenkel, A. I.; Crooks, R. M. *Langmuir* **2010**, *26*, 1137.
- (31) Teng, X. W.; Wang, Q.; Liu, P.; Han, W.; Frenkel, A.; Wen, W.; Marinkovic, N.; Hanson, J. C.; Rodriguez, J. A. *J. Am. Chem. Soc.* **2008**, *130*, 1093.
- (32) Herzing, A. A.; Carley, A. F.; Edwards, J. K.; Hutchings, G. J.; Kiely, C. J. *Chem. Mater.* **2008**, *20*, 1492–1501.
- (33) Liu, H. B.; Pal, U.; Medina, A.; Maldonado, C.; Ascencio, J. A. *Phys. Rev. B* **2005**, *71*.
- (34) Ferrer, D.; Torres-Castro, A.; Gao, X.; Sepulveda-Guzman, S.; Ortiz-Mendez, U.; Jose-Yacamán, M. *Nano Lett.* **2007**, *7*, 1701.

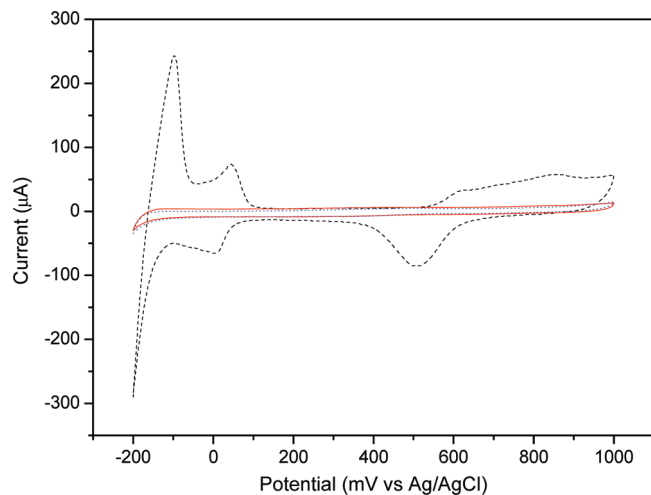


Figure 1. CVs recorded on Pd/C (dash line), PdAu/C (solid line), and PdAu/C after a continuing decomposition reaction of 30 h (dot line) coated electrodes in N_2 -saturated 0.5 M H_2SO_4 solution at a potential scan rate of 20 mV S^{-1} .

N_2 for 15 min in order to remove the dissolved oxygen before cyclic voltammogram (CV) was recorded. CO stripping voltammograms were also recorded in an aqueous solution of 0.5 M H_2SO_4 . For CO adsorption on the catalyst, the CO gas was purged into the solution for 40 min in order to allow the complete adsorption of CO onto the catalyst-coated electrode that was controlled at 100 mV. The solution was then bubbled with a pure N_2 for another 40 min to remove the dissolved CO. At last, the stripping voltammograms were recorded.

Analysis for Formic Acid Decomposition. The reaction was performed in a test tube containing 5 mL of 6.64 M formic acid, 6.64 M sodium formate, and 60 mg of catalyst at 92°C . The temperature was controlled by an ultraprecise thermostat bath (Shanghai Instrument, China). Then the reforming gases from this reaction bath were collected by an injector, as described in the literature.³ To examine the catalytic stability of the PdAu/C catalyst, we also carried out a continuing reaction of 30 h. The long time reaction was performed with 10 mg of PdAu/C catalyst and 60 mL of solution containing 6.64 M formic acid and 6.64 M sodium formate at a temperature of 92°C . The catalyst after the long reaction time was washed with the hot triply distilled water and then dried in a vacuum at 80°C overnight. The obtained catalyst was used for characterization without other treatment. For the recycling experiment, the PdAu/C catalyst in the test tube was filtered and washed with the hot triply distilled water after a full conversion of formic acid. Then, it was dried in air at 80°C for 3 h. The formic acid decomposition for the recycled catalyst was also performed in a test tube containing 5 mL of 6.64 M formic acid, 6.64 M sodium formate, and 60 mg of catalyst at a temperature of 92°C .

Results and Discussion

Structural Characterizations of the PdAu/C. The electrochemical measurements were first used to characterize the surface composition of the prepared PdAu/C catalyst.²¹ In general, there are hydrogen adsorption/desorption waves for Pd surface if using a cyclic voltammetry technique. In other words, if the surface of a catalyst contains Pd, its CV should show the hydrogen adsorption/desorption waves. Figure 1 shows the CVs of

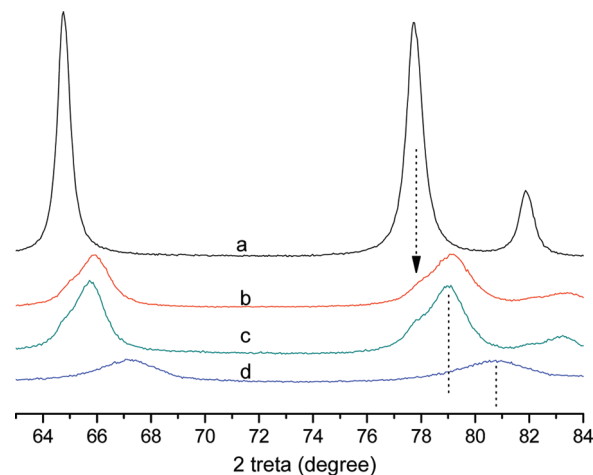


Figure 2. XRD patterns of (a) Au/C, (b) PdAu/C, (c) PdAu/C after a continuing decomposition reaction of 30 h and (d) Pd/C.

Pd/C and PdAu/C coated electrode in a N_2 -saturated 0.5 M H_2SO_4 solution. For the Pd/C coated electrode, the large hydrogen adsorption/desorption waves in the potential range of -0.2 to 0.1 V can be clearly observed. However, the PdAu/C-coated electrode has no hydrogen adsorption/desorption waves, which means that the surface of the PdAu/C material does not contain Pd element. Furthermore, the absence of redox peaks of Pd element also demonstrates that there are no Pd atoms on the surface of PdAu/C. Then, there appears a question about the bimetallic material. Where is the Pd element? To answer this question, we carried out ICP-OES to analyze the chemical components in the PdAu/C sample. The Pd and Au loading in the whole sample are detected to be 10.1 and 57.0 wt % in sequence, which are close to those expected loading on the basis of the metal precursors in the preparation. Exactly, Pd element exists in the prepared bimetallic material. It can then be deduced that there is a core-shell structure in the PdAu/C. The shell is composed of Au only, whereas Pd should be located in the core.

To clarify the internal structure of the PdAu/C, the XRD analysis was achieved. Figure 2 shows the XRD results of the prepared Au/C, Pd/C, and PdAu/C catalysts. The patterns all correspond to face-centered cubic phase structures. For example, the 2θ values of 65.9 , 79.1 , and 82.0° in Figure 2a can be indexed to the diffraction of (220), (311), and (222) planes of Au, respectively. For the PdAu/C material, the pattern exhibits some broad but well-defined diffraction peaks in the position between the corresponding Au and Pd peaks, indicating that the formation of PdAu alloy in the catalyst. In other words, the core is a Pd and Au alloyed material because of the absence of Pd in the shell. Then, the core-shell structure with an alloyed PdAu core and an Au shell in the obtained PdAu bimetallic material is confirmed evidently and defined as PdAu@Au/C. In addition, a weak shoulder peak at the position of Au diffraction can also be observed in the XRD pattern of the PdAu/C sample, which may be attributed to those thick Au shells and a minor population of pure Au particles in the catalyst. Generally,

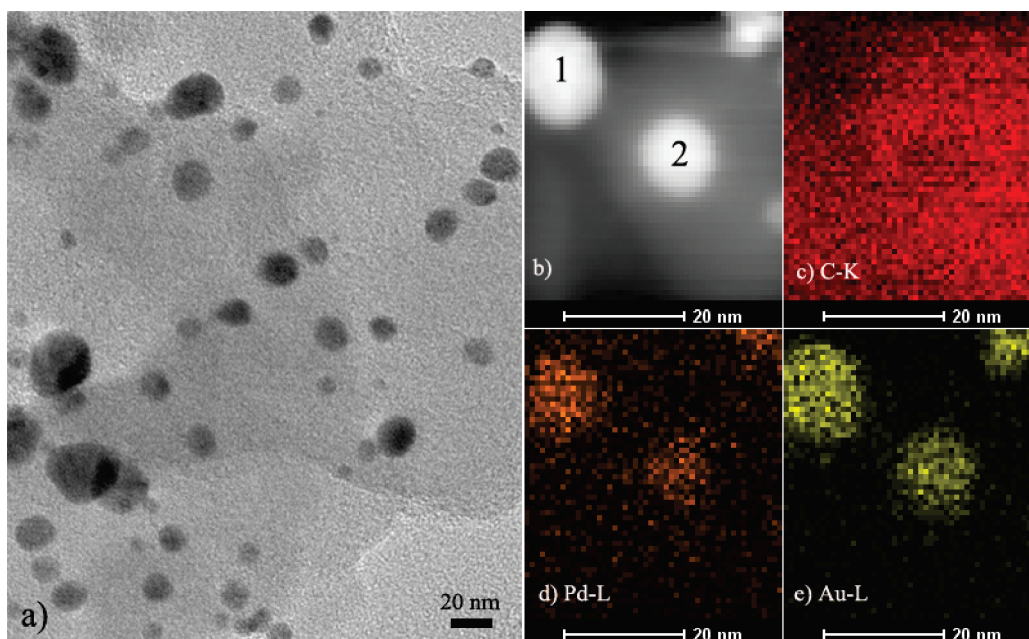
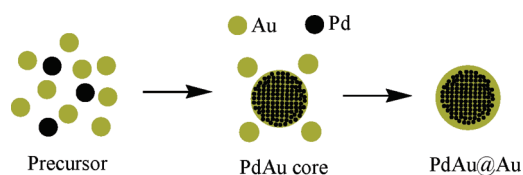


Figure 3. (a) TEM image of the prepared PdAu/C. (b) HADDF-STEM image of the particles from the PdAu/C. (c–e) Corresponding EDS mapping images of b for C, Pd, and Au elements, respectively.

the core of a bimetallic core–shell structure can be detected by XRD because the core diameter is always large enough to give significant diffraction peaks. However, whether the XRD diffraction of the shell is detectable depends on the thickness of the shell.^{35–38} For example, the Pd shell with a thickness of 0.8 nm was too thin to make significant peaks of XRD while the diffraction peaks of the Pd shell with a thickness of 3 nm could be seen distinctly for the Au@Pd core–shell structure.^{37,38} In the prepared PdAu@Au/C catalyst, there may be some of thick Au shells that can give diffraction peaks. On the other hand, a small quantity of Au particles may be formed in the preparation procedure because the abundant Au precursors are used. Then, the shoulder peak of Au may be attributed to the accumulation of diffractions from the above two kinds of Au. The detailed chemical components in the internal structure are also analyzed by using the XRD results. The diffraction peak of (220) is far from the background signal of carbon support and then chosen for the calculation of lattice constant. The lattice constants of the metallic crystallites are calculated to be 4.067, 3.937, and 4.006 Å for the Au/C, Pd/C, and PdAu/C catalyst, respectively. According to Vegard's law, the molar fraction of Pd in the PdAu/C is estimated to be 0.45, which is larger than that in the whole catalyst. The result is reasonable because a portion of Au atoms are located in the shell and not alloyed with Pd.

The morphologic measurements of synthesized PdAu@Au/C catalyst was also assessed to reveal further the microstructure. Figure 3a shows a TEM image of the obtained

Scheme 1. Suggested Growth Process of PdAu@Au



PdAu@Au/C catalyst. It can also be seen that the metal particles are well-dispersed on the carbon support and are not uniform. The size distribution from the TEM image exhibits that about three-quarters of the particles are in the size range of 10–20 nm and the average size is about 16 nm. As shown in the STEM-HADDF image of Figure 3b and the corresponding EDS maps, Au atoms are distributed in the whole particles, whereas Pd atoms are mainly located in the center of the particles. This indicates clearly that the particles have a core–shell nanostructure with an alloyed PdAu core and an Au shell. For the particle 1, the core diameter and shell thickness are about 15.4 and 1.5 nm, respectively. However, the particle 2 has a core diameter of 12.1 nm and shell thickness of 2.0 nm. It is suggested that both the shell thicknesses and the core sizes of the particles may be not homogeneous and change from particle to particle. Therefore, the EDS analysis of only two particles was given as an example to display the microstructure of the sample. Obviously, the morphologic observations agree well with the above electrochemical and XRD results.

Although the detailed mechanism for the formation of the PdAu@Au/C core–shell particles may be complicated, a phenomenological growth procedure is proposed and shown in Scheme 1. The Pd atoms are first alloyed with Au atoms to form alloy particle as the reduction reaction takes place. The abundant Au ions are then deposited onto the preformed alloy particle, forming a

- (35) Jose, D.; Jagirdar, B. R. *J. Phys. Chem. C* **2008**, *112*, 10089.
 (36) Jana, D.; Dandapat, A.; De, G. *J. Phys. Chem. C* **2009**, *113*, 9101.
 (37) Mizukoshi, Y.; Okitsu, K.; Maeda, Y.; Yamamoto, T. A.; Oshima, R.; Nagata, Y. *J. Phys. Chem. B* **1997**, *101*, 7033.
 (38) Harpeness, R.; Gedanken, A. *Langmuir* **2004**, *20*, 3431.

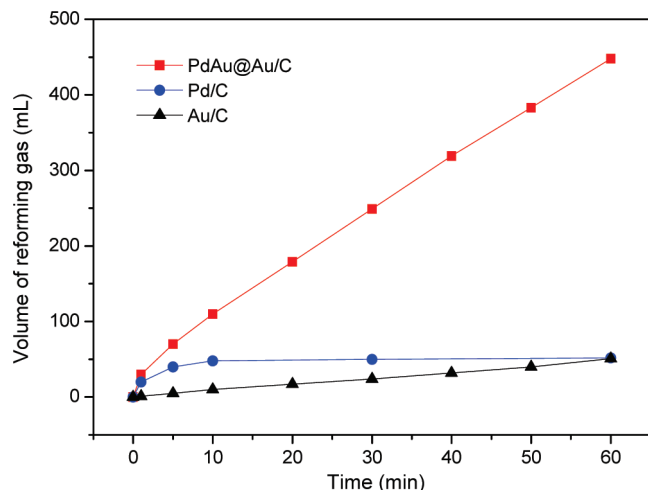


Figure 4. Volume change of reforming gas with time for 60 mg of the synthesized catalyst in 5 mL of solution containing 6.64 M formic acid and 6.64 M sodium formate at a reaction temperature of 92 °C.

core–shell structure with an Au shell and a PdAu alloy core. The simultaneous reduction method was not commonly used to prepare core–shell structure because it was hard to control the preformed core and the subsequent deposit of shell. To obtain core–shell structure using the simultaneous reduction method, mild reduction conditions in the presence of stabilizing agents were commonly required.^{9,25} In our research, it is interesting that the PdAu@Au core–shell structure is formed in the strong reduction condition without any stabilizer. One reason may be the high miscibility of Pd and Au, which can be seen from their phase diagrams. The other reason may be the proper molar ratio of metal precursors in this study.

PdAu@Au/C-Catalyzed Formic Acid Decomposition to Generate Hydrogen. The core–shell bimetallic catalyst and the monometallic catalysts were used for the catalytic decomposition of formic acid and the obtained results are shown in Figure 4. It can be seen that the Pd/C catalyst is active for the decomposition reaction at the beginning. Nevertheless, there is a distinct deactivation effect after 10 min, which may result from the formation of poisoning intermediates on the catalyst surface as the decomposition reaction goes on. Although the deactivation phenomenon has not been observed on the Au/C catalyst, the catalytic activity of Au/C is very low. For example, the output rate of reforming gas is only 0.8 mL min⁻¹. When the Pd and Au was constructed to a core–shell structure of PdAu@Au/C, the volume of obtained reforming gas increases sharply at the beginning and then continues to increase linearly at a fast rate of about 7.1 mL min⁻¹. The rate is almost nine times higher than that on the Au/C catalyst. It demonstrates that the core–shell structure is very active for the decomposition of formic acid. For the PdAu@Au/C catalyst, the selectivity of the formic acid decomposition was also examined. The CO content of the reforming gas from the decomposition reaction of 1 h was determined to be 30 ppm by FT-IR spectroscopy (see Figure S1 in the Supporting Information). It indicates that the PdAu@Au/C catalyst can restrain the CO

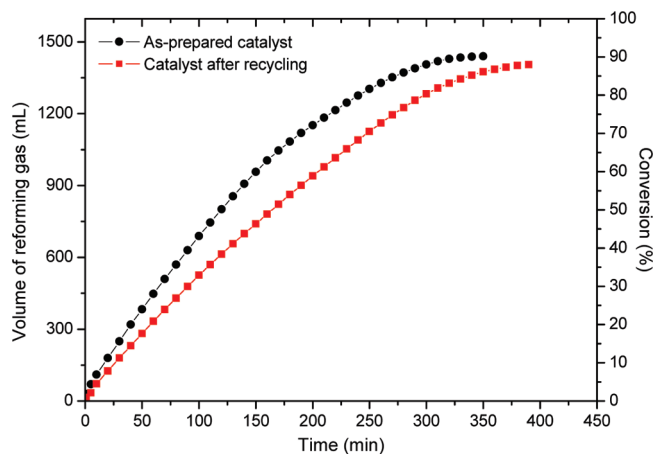


Figure 5. Formic acid decomposition from 5 mL of solution containing 6.64 M formic acid and 6.64 M sodium formate using 60 mg as-prepared PdAu@Au/C catalyst and the PdAu@Au/C catalyst after recycling at a reaction temperature of 92 °C.

formation and promote the dehydrogenation pathway for the formic acid decomposition.⁸ The high selectivity is very important for the hydrogen generation because the reforming gas with a low content of CO is always a favor in fuel cell applications. Especially, the prolonged reaction and gas collection were also carried out to observe the conversion of formic acid as the core–shell catalyst was used in the decomposition reaction. As shown in Figure 5, a conversion of about 90% can be achieved after the reaction goes on for about 6 h.

Regarding the improved catalytic performance of formic acid decomposition, we believe that the enhanced decomposition rate of formic acid on PdAu@Au/C catalyst might be related to the special core–shell structure of this catalyst when compared to that on Pd/C and Au/C catalyst. This core–shell structure should have a much stronger tolerance to CO adsorption than that of monometallic catalyst such as Pd which is easy to be poisoned by CO. To confirm this, the CO adsorption and stripping experiments were carried out using both Pd/C and PdAu@Au/C-coated electrodes. As shown in Figure 6, both the onset potential and the peak area of CO oxidation for the PdAu@Au/C are very low as compared with those for the Pd/C catalyst, which indicates that the PdAu@Au/C catalyst has a strong capability of antipoisoning of CO. The result is consistent with that of the recent theoretical research, in which the Au-rich surface in the Au–Pd bimetallic system is speculated to have a high activity of antipoisoning toward CO.³⁹ For such a significant CO-tolerance capability of core–shell PdAu@Au/C catalyst, the detailed relationship between the core–shell structure and the catalytic activity needs to be further investigated and is our ongoing research.

Stability Test of the PdAu@Au/C Catalyst. The catalytic stability of the core–shell catalyst was also examined by a continuing decomposition reaction. As shown in Figure 7, the catalytic activity of the PdAu@Au/C catalyst does not decrease after 30 h of reaction, which

(39) Zhang, J.; Jin, H. M.; Sullivan, M. B.; Chiang, F.; Lim, H.; Wu, P. *Phys. Chem. Chem. Phys.* **2009**, *11*, 1441.

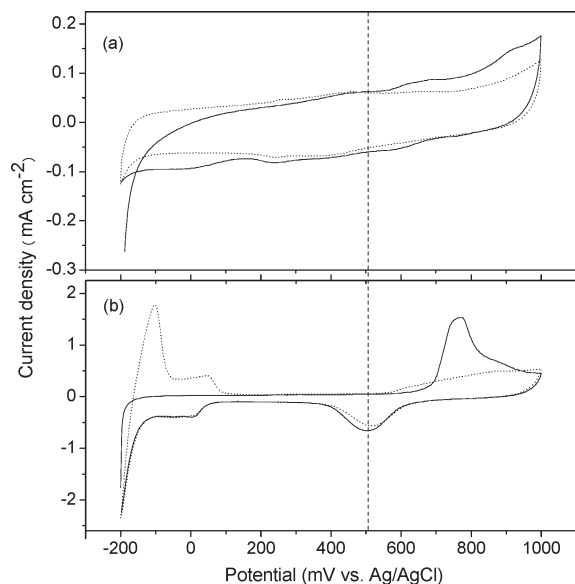


Figure 6. CO_{ad} stripping voltammograms of (a) PdAu@Au/C and (b) Pd/C with a scan rate of 20 mV s^{-1} .

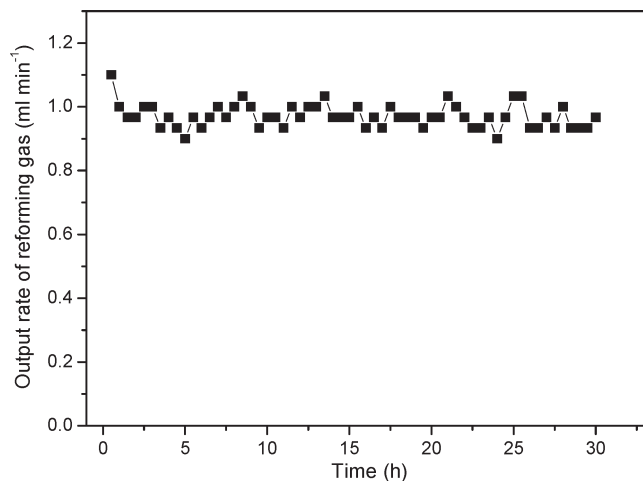


Figure 7. Catalytic stability test of 10 mg of PdAu@Au/C in 60 mL of solution containing 6.64 M formic acid and 6.64 M sodium formate at a temperature of 92°C .

demonstrates the high catalytic stability of the core-shell catalyst. To check the selectivity for the long time reaction, the CO content of the reforming gas after the reaction of 30 h was also detected. Result shows that the CO content is about 34 ppm (see Figure S1 in the Supporting Information) and comparable with that for the short time reaction. In the previous research, it was found that there is an effect of formate/formic acid on the CO content of reforming gas.³ It should be pointed that this effect could be very low in the long time reaction because only about 10% of the formic acid has been consumed. It is then concluded that there is no influence on the selectivity for the long time reaction. The composition and structure of the core-shell catalyst after the long time reaction was also characterized. The results of the ICP-OES analysis show that the Pd and Au loading in the whole catalyst after use are examined to be 10.2 and 56.9 wt %, respectively, which is almost the same to

those in the catalyst before use. This indicates that the PdAu catalyst does not dissolve into the reactant solution during the reaction. The CV in Figure 1 of the catalyst after use does not show the characteristic hydrogen adsorption/desorption waves, indicating the absence of Pd in the catalyst surface. As shown in Figure 2c, the existence of PdAu alloy in the internal structure can also be proved by the XRD pattern. The molar fraction of Pd in the alloy is calculated to be 42% by using the lattice constant and Vegard's law. The value agrees well with that in the catalyst before reaction. These results indicate that the catalyst after use contains also a core-shell structure of PdAu@Au. In addition, the composition in both the whole catalyst and the internal structure has not been changed after the long time reaction. Obviously, the observed high catalytic stability is attributed to the high stability of the core-shell structure. It has been found that Pd atoms have a tendency to migrate to the exterior surface of the PdAu bimetallic materials, which is driven by the preferential oxidation of Pd relative to Au under the heat treatment in the atmosphere.^{32,40} In our research, the core-shell structure of PdAu@Au is very stable even after long time reaction. The reasons for the absence of the migration effect could be 2-fold: (a) the strong reduction condition in the reaction and (b) the low temperature of the reaction. The reactant solution of formic acid is a strong reducing agent and can prevent the oxidation of metal. Thus, the driven force for the migration can be greatly decreased. In addition, the temperature for our reaction is near-ambient and only 92°C , which is much lower than the elevated temperature given for the observation of the migration effect.³² Notably, a recycling experiment after separation of the core-shell catalyst was also presented. As shown in Figure 5, about 88% of formic acid has been converted within 7 h. It indicates that the catalyst after recycling is still active.

Conclusions

In summary, it was found that a core-shell structured PdAu@Au can be prepared by a simultaneous reduction method without any stabilizing agents. The novel nanostructure was supported on carbon and successfully used as the catalyst for hydrogen generation from formic acid decomposition. It was significant to find that the catalyst exhibited high activity, high selectivity, and stability at a low temperature. The catalytic performance was much better than that for the corresponding monometallic catalysts. Especially, the reforming gas from formic acid decomposition contained only 30 ppm of CO and can be used directly to feed the fuel cells. This study proposed a novel bimetallic structure and could open an effective method for hydrogen generation from renewable fuels such as formic acid.

(40) Edwards, J. K.; Solsona, B.; Landon, P.; Carley, A. F.; Herzing, A.; Watanabe, M.; Kiely, C. J.; Hutchings, G. J. *J. Mater. Chem.* **2005**, *15*, 4595.

Acknowledgment. The authors acknowledge financial support by High Technology Research Program (863 program, 2007AA05Z159 and 2007AA05Z143) of Science and Technology Ministry of China and the National Natural Science Foundation of China (20703043 and 20933004). The authors are also grateful for the help of Yunchun Zhou,

Lijin Zhang, Hanwu Dong, Wenbing Xie, and Dongmei Wang.

Supporting Information Available: FT-IR spectra for CO detection (PDF). This material is available free of charge via the Internet at <http://pubs.acs.org>.